

Cite this: *CrystEngComm*, 2012, **14**, 1920

www.rsc.org/crystengcomm

COMMUNICATION

Hydrothermal synthesis of rutile TiO₂ nanoflowers using Brønsted Acidic Ionic Liquid [BAIL]: Synthesis, characterization and growth mechanism†Sawanta S. Mali,^a Chirayath A. Betty,^b Popatrao N. Bhosale,^c Rupesh S. Devan,^d Yuan-Ron Ma,^d Sanjay S. Kolekar^a and Pramod S. Patil^{*a}

Received 3rd November 2011, Accepted 9th January 2012

DOI: 10.1039/c2ce06476f

Herein we report a facile method to synthesize rutile TiO₂ nanoflowers (TNF) comprising a bunch of aligned nanorods with uniform size and shape *via* a hydrothermal method in Brønsted Acidic Ionic Liquid [BAIL] room temperature ionic liquid (RTIL). This method has some advantages: the process is simple and single step; the reaction can be performed under low temperature. The TNFs are highly crystalline and free of aggregation.

Many hierarchical one-dimensional (1D) semiconductor nanostructures such as nanorods, nanowires and nanotubes are receiving much attention because of their unusual properties rather than bulk. Specially, oriented single-crystalline TiO₂ nanorods (TNR) or nanowires (TNW),^{1,2} microspheres,³ nanotubes (TNT)⁴ and nanocorals (TNC)^{5,6} would be most desirable, but achieving these structures is a challenging task. Synthesis of aligned nanowire arrays is a critical step toward enhancing nanostructure performances in nanoscale devices. Compared to ZnO, symmetry and crystal structure of TiO₂ (either anatase or rutile), makes growth of oriented anisotropic single crystalline TiO₂ thin films very difficult. We describe a single-step synthesis of rutile TiO₂ nanoflowers (TNF) comprising a bunch of aligned nanorods in room temperature ionic liquids (RTIL). The high thermal stability, negligible vapor pressure, wide electrochemical window, no combustion, non-toxicity, and unusual dissolving capability of RTIL are widely explored in various applications especially in the field of organic synthesis, catalysis, separation and good solvents for dye sensitized solar cells (DSSCs).⁷ Many attempts have been made for controlling the morphology of TiO₂ using different techniques which includes electrodeposition,⁸

solvothermal⁸ and hydrothermal,⁹ anodization¹⁰ template based growth sol-gel electrophoresis,¹¹ and by using different surfactants.¹² Many inorganic nanostructures,^{13,14} including TiO₂,^{15–20} have been fabricated *via* various IL-involved processes. For titania nano-materials, however, to the best of our knowledge, few studies about the synthesis of rutile nanostructures have been reported in IL solutions.^{21,22} Recently, Kunlun Ding *et al.* successfully developed a route for the synthesis of high quality TiO₂ nanocrystals in ionic liquid *via* a microwave-assisted process.^{23–25}

Bin *et al.* have reported the effects of temperature, initial reactant concentration, titanium precursor and acidity for the growth of TiO₂ nanorods. The study concluded that the equal volume proportion of H₂O and HCl is favorable for growth of well aligned TiO₂ nanorods.²⁶ Therefore, we choose equal volumes of concentrated HCl and H₂O, which is the requirement for slow hydrolysis of TTIP. In a typical synthesis, titanium(IV) isopropoxide (0.5 mL) was added to an equal volume of distilled water and concentrated HCl. The resulting mixture was stirred for 30 min. The clear transparent solution was then transferred to a Teflon-lined stainless steel autoclave (25 mL), and a piece of glass was immersed in the solution parallel to the wall. The autoclave was sealed and placed in an oven at 180 °C for 3 h. After cooling the autoclave to room temperature, the TiO₂ films were washed several times with distilled water and dried in an oven at 70 °C for 1 h and the sample was designated as TNR. In this reaction, the (110) planes of rutile TiO₂ could be retained due to the relatively slow growth rate for the O^{2–} terminated planes in comparison to other crystal planes. For preparing TiO₂ nanoflowers (TNF), we used 0.5 mL (in 25 mL of H₂O : HCl) RTIL, 1 : 3-ethoxycarbonyl-ethyl-1-methyl-imidazolium chloride [CMIM][HSO₄], titanium isopropoxide (TTIP) and concentrated HCl as a precursor in distilled water for the synthesis of TNR. (Please see ESI† S1 for synthesis of [CMIM][HSO₄] RTIL). The autoclave was sealed and placed in an oven at 180 °C for 3 h. After cooling the autoclave to room temperature, the TiO₂ films were washed several times with distilled water and dried in an oven at 70 °C for 1 h and the sample was designated as TNF. The morphology of the prepared TiO₂ samples was characterized by the scanning electron microscopy (SEM, JEOL-JSM-6360 operated at 20 keV). The structural properties of the TiO₂ films were studied from X-ray diffraction (XRD) patterns recorded using an X-ray diffractometer (Philips, PW 3710, Almelo, Holland) operated at 25 kV,

^aThin Film Materials Laboratory, Department of Physics, Shivaji University, Kolhapur, India 416 004. E-mail: psp_phy@unishivaji.ac.in; sawantamali@yahoo.co.in; Fax: +91-0231-2691533; Tel: +91-231-2609229

^bChemistry Division, Bhabha Atomic Research Center (BARC), Trombay-Mumbai, India 85

^cMaterials Research Laboratory, Department of Chemistry, Shivaji University, Kolhapur M. S, India 416004

^dDepartment of Physics, National Dong Hwa University, Hualien, 97401, Taiwan, Republic of China

† Electronic supplementary information (ESI) available: S1-synthesis of [BMIM][HSO₄] RTIL, S2-SEM and FESEM images of TNR, S3-SEM and FESEM images of TNF, S4-XRD spectra of TNR and TNF. See DOI: 10.1039/c2ce06476f

20 mA with Cu-K α radiation ($\lambda = 1.5406 \text{ \AA}$). The Raman spectra of the films were recorded in the spectral range of 36–3600 cm^{-1} using Fourier-Transform Raman spectrometer (Bruker Multi-RAM, Germany Make) Nd:YAG laser source with excitation wavelength of 1064 nm and resolution 4 cm^{-1} at 336 mW laser power. Fig. 1 shows the FESEM images of TNR prepared by hydrothermal route. Most of structures displayed microspheres containing nanorods of $\sim 250 \text{ nm}$ diameter. It is suggested that because of the complete miscibility of water and HCl with the TTIP, microspheres containing $\sim 250 \text{ nm}$ sized nanorods are formed during the hydrothermal process. The nanorods are nearly perpendicular to the glass substrate. The nanorods are tetragonal in shape with square top facets, the expected growth habit for tetragonal crystal structures. Fig. 2 shows the TiO_2 nanoflowers with petals comprising a bunch of aligned nanorods, prepared in RTIL. It retains the rod like array geometry but the nanorod diameter drastically decreased to $\sim 62 \text{ nm}$. Scheme 1 illustrates the mechanism for the aligned nanorods and nanoflowers formation. More SEM and FESEM images of TNR and TNF are available in Fig. S2 and S3 in the ESI.†

When the longer-chained 1 : 3-ethoxycarbonyl-ethyl-1-methylimidazolium chloride $[\text{CMIM}][\text{HSO}_4]$ RTIL is employed,

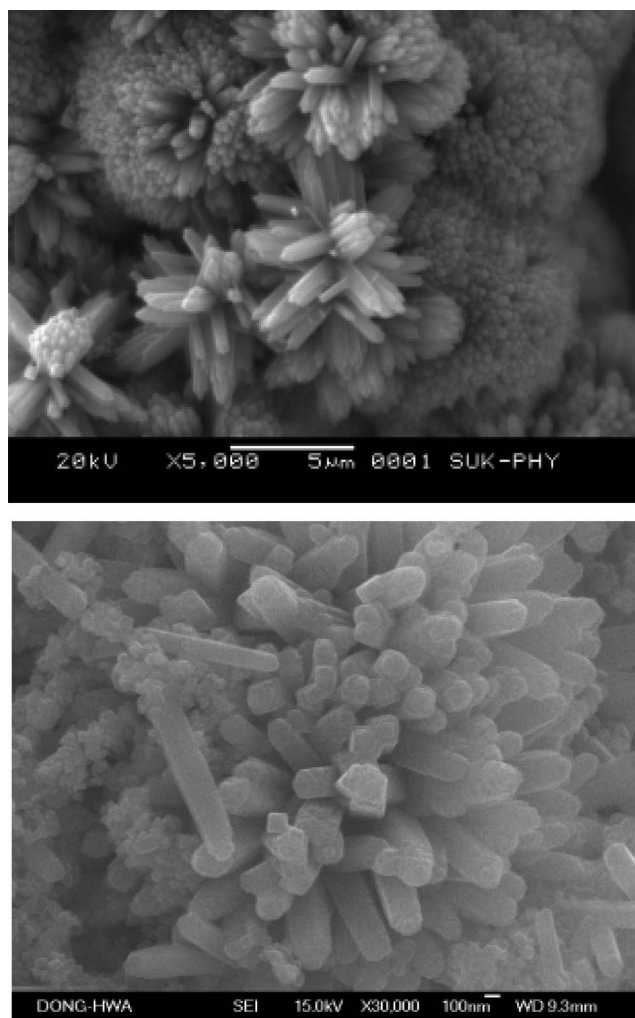


Fig. 1 SEM images shows TNR at different magnifications of (a) 5000 and (b) 25 000.

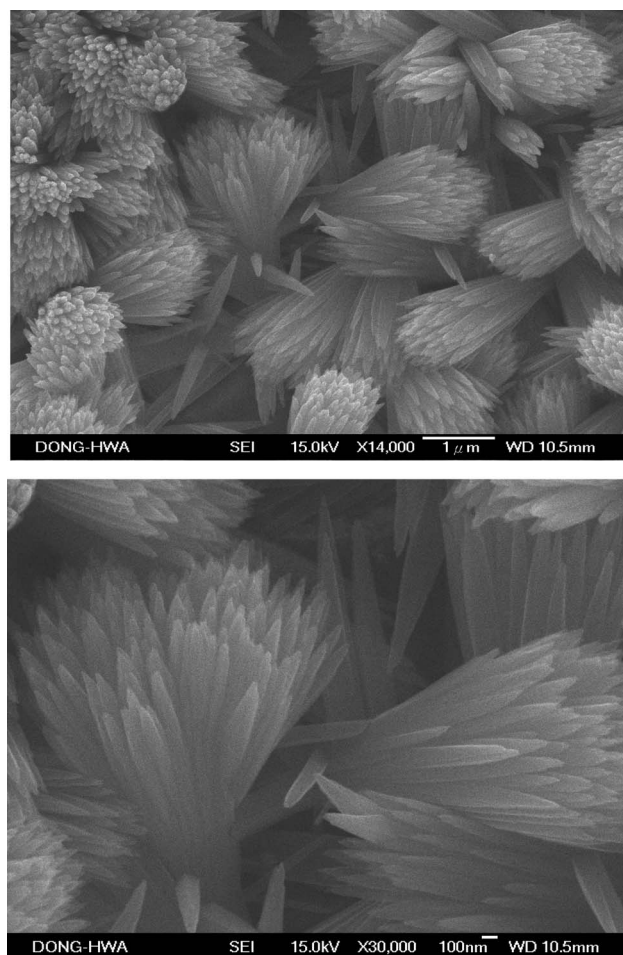
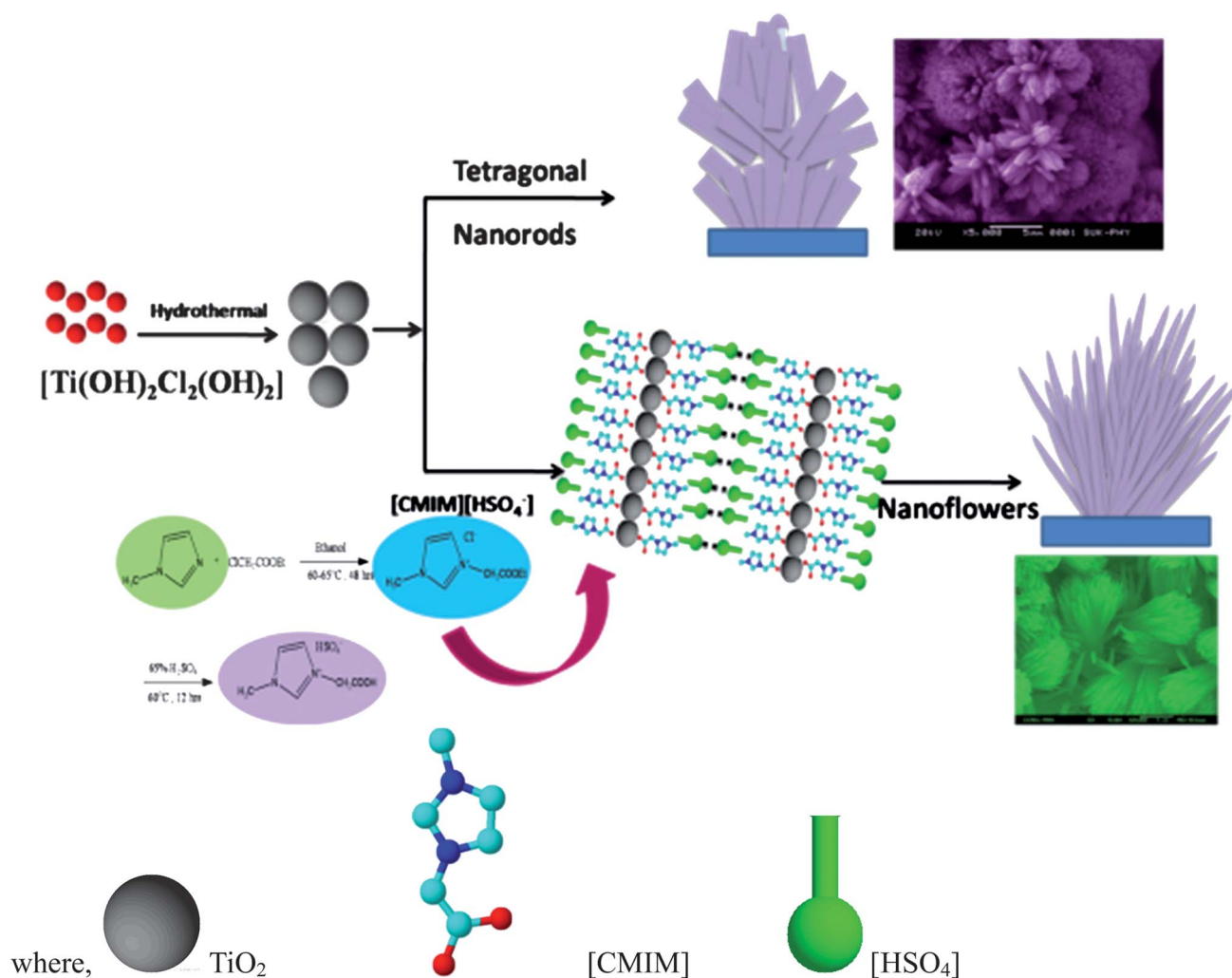


Fig. 2 FESEM images shows TNF at different magnifications of (a) 14 000 and (b) 30 000.

nanoflowers comprising a bunch of aligned nanorods were obtained. The ionic liquid content in the precursor solution controlled formation of regular, titania aligned nanorod arrays having $\sim 62 \text{ nm}$ size. This is due to the fact that a presence of 3-carboxymethyl-1-methylimidazolium bisulfate $[\text{CMIM}][\text{HSO}_4]$ can effectively control the gathering of the nanoparticles and improve the dispersion in the reaction system just like a surfactant. Because the RTIL can cap the surface of the nanocrystals, it provides a low agglomeration tendency, good dispersibility and the potential to tailor the surface properties. Furthermore, RTILs can form extended hydrogen bond systems in the liquid state resulting in highly structured TNF. The $[\text{CMIM}]^+$ ions are separated in accordance with the mutual π -stacking distance (0.6–0.7 nm) between the aromatic rings. So we suggest that the $[\text{CMIM}]^+$ cations facilitates the optimized relocation of the molecules based on its ability to self-assemble into ordered structures, stabilized by additional π - π^* interactions between the methylimidazolium rings of $[\text{CMIM}][\text{HSO}_4]$.

It is suggested that, two particular properties of $[\text{CMIM}][\text{HSO}_4]$ enhance the growth of rutile TNF containing a bunch of aligned nanorods. Firstly, as molten salts, $[\text{CMIM}][\text{HSO}_4]$ ions promote the ionic strength by dissolving in solution and consequently enhancing the solubility of the Ti species. After the formation of $[\text{Ti}(\text{OH})_2 \cdot \text{Cl}_2(\text{OH})_2]$ growth units of titania nanocrystals grow at step edges proceeded by the addition of Ti species. Secondly, although polar,



Scheme 1 Schematic illustration for the growth process of the TNRs and TNFs

$[\text{CMIM}][\text{HSO}_4]$ can serve as efficient surfactants by dissolving in solution to form steady solutions, and then cap on the nanocrystal facets to enhance the orientation of particles after rutile particles were formed.

It also offers excellent ionic strength to the growth solution which favors the formation of small crystals through electrostatic screening which is not available in traditional surfactants. Fig. 3 (a) shows the selected area electron diffraction (SAED) pattern of the TNF sample. The SAED pattern of the rutile crystal shows a spot pattern which indicates a single-crystalline nature of the rutile TiO_2 nanorods.^{27,28} The XRD pattern of TiO_2 with and without RTIL, which matches well with the standard pattern of tetragonal rutile phase (SG, $P4_2/mnm$; JCPDS-08-4920, $a = b = 4.53 \text{ \AA}$ and $c = 2.92 \text{ \AA}$) that are free of anatase and brookite impurities. Compared to the XRD pattern of TNR, the (110) diffraction peak of TNF was significantly broadened, ESI† S4-XRD). The formation of the dark spot pattern indicates the single crystalline nature of the sample.

The clear lattice fringe of the single nanorod of the nanoflower sample is observed to be single crystalline along their entire length. The interplanar spacings obtained from the HRTEM lattice fringes of TNF (Fig. 3), $d_{110} = 3.3 \pm 0.1 \text{ \AA}$ between the adjacent lattice fringes perpendicular to the rod axis can be assigned to the rutile TiO_2 (110). The lattice spacing of $d_{001} = 2.9 \pm 0.1 \text{ \AA}$ along the longitudinal

axis direction pertains to the d-spacing of rutile TiO_2 (001) crystal planes. This indicates the formation of a single crystalline rutile phase, in agreement with the XRD results (ESI† S4).

First-order Raman spectra of rutile TiO_2 shows four Fourier Transform (FT) Raman active fundamental modes at $143 (\text{B}_{1g})$, $447 (\text{E}_g)$, $612 (\text{A}_{1g})$, and $826 \text{ cm}^{-1} (\text{B}_{2g})$ expressed as $\text{A}_{1g} + \text{B}_{1g} + \text{B}_{2g} + \text{E}_g$. For the rutile phase, two prominent maxima at $445 (\text{E}_g)$ and $609 \text{ cm}^{-1} (\text{A}_{1g})$, are comparable with that found in the rutile TiO_2 single crystal (Fig. 4). In addition, there are second-order scattering features, the most prominent one at $\sim 237 \text{ cm}^{-1} (\text{E}_g)$ peak due to the multiple-phonon scattering processes, which is also considered as a characteristic Raman peak of rutile type TiO_2 .²⁹ In the Raman spectra of our samples, the E_g and A_{1g} modes, as well as the second-order effect at $\sim 237 \text{ cm}^{-1}$, are the major features; the B_{1g} and B_{2g} modes are extremely weak or absent. With conversion from TNRs to TNFs, the wavenumber of all peaks decreased relevantly; in particular, the E_g (612 cm^{-1}) mode shifted by about 6 cm^{-1} , while the intensity of second order E_g mode ($\sim 237 \text{ cm}^{-1}$) is drastically increased.

The second order E_g at 237 cm^{-1} , a characteristic of rutile TiO_2 , is more intense and slightly broader and shifted with respect to that of a TNR sample. This nature is due to the phonon confinement effect in which the decrease in the particle dimensions to the nanometre scale can cause a wave number blue shift and broadening of Raman peaks.³⁰

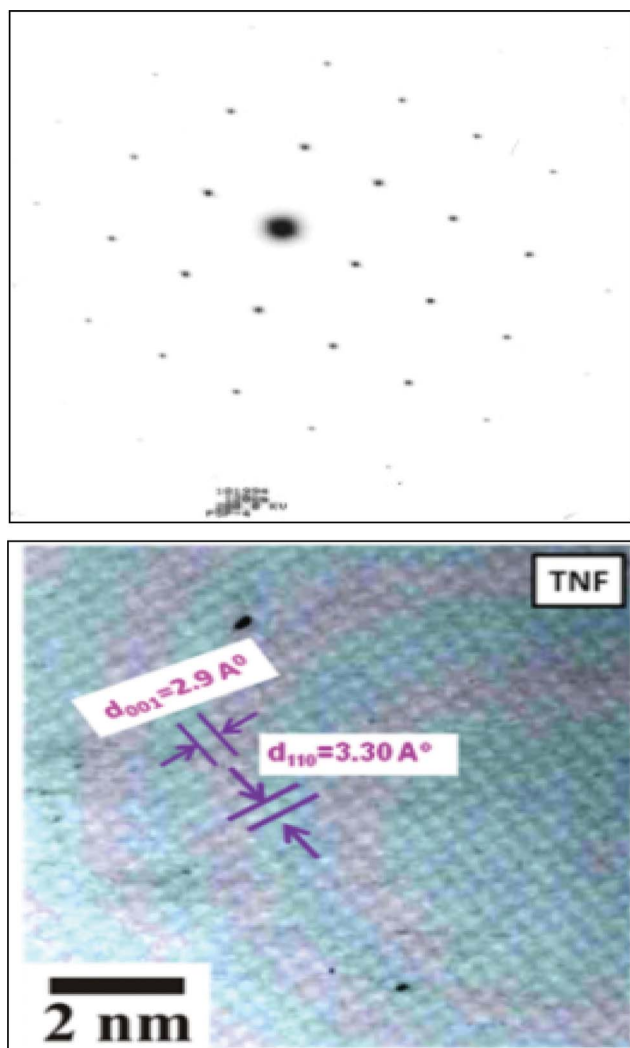


Fig. 3 (a) SAED pattern of the TNFs. (b) High magnification TEM image of the TNFs.

The non-linear behavior of the E_g peak intensity suggests strong light scattering differences among samples, potentially related to changes on the morphological properties of the TNR and TNF.

In conclusion, we have demonstrated a facile way for synthesis of novel TiO_2 nanoflowers (TNF) using ecofriendly $[\text{CMIM}][\text{HSO}_4]$ RTIL by single step hydrothermal process. The addition of $[\text{CMIM}][\text{HSO}_4]$ ionic liquid to the synthesis of rutile TiO_2 results in a favourable route to form a 1D nanostructure, in particular, nanoflowers. Furthermore, $[\text{CMIM}][\text{HSO}_4]$ helped to achieve a high degree of crystallization even at mild annealing temperatures, such as 180°C . These TNF may be useful for basic studies on size-and shape-dependent properties of TiO_2 . This method will open up a new approach to develop hierarchical functional nanomaterials such as TiO_2 using ionic liquid. There are hardly any reports on the preparation of small size (~ 60 nm), well oriented, highly crystalline TiO_2 nanoflowers (TNF) using room temperature ionic liquids. It is envisaged that such a simple and mild route could also be extended to prepare other hierarchical nanostructured metal oxides like ZnO , SnO_2 , and WO_3 etc. with small size nanostructures. The hierarchical, highly crystalline and oriented nanostructures thus promise potential applications for improving the DSSC photoconversion efficiency by increased light harvesting, better

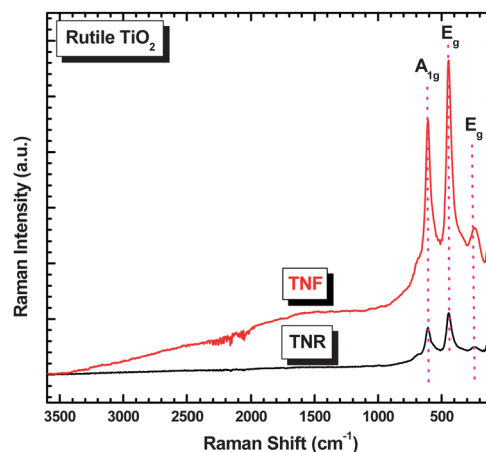


Fig. 4 FT-Raman spectra of synthesized TNR and TNF.

dye contact and decreased carrier recombination. Further studies are being carried out to confirm the advantages.

Acknowledgements

One of the authors (SSM) wish to acknowledge DAE-BRNS Mumbai for financial support through the DAE-BRNS project no. 2008/37/8/BRNS/1489 for the 2008–2012. Authors are very much thankful to Mr. P.P. Salvi and Dr S.S. Kolekar, Department of Chemistry, Shivaji University Kolhapur for availing the $[\text{CMIM}][\text{HSO}_4]$ room temperature ionic liquid.

Notes and references

- 1 C. Sun, N. Wang, S. Zhou, X. Hu, S. Zhou and P. Chen, *Chem. Commun.*, 2008, 3293.
- 2 D. R. Baker and P. V. Kamat, *Adv. Funct. Mater.*, 2009, **19**, 805.
- 3 S. S. Mali, C. A. Betty, P. N. Bhosale and P. S. Patil, *CrystEngComm*, 2011, **13**, 6349.
- 4 K. Gopal, V. O. K. Mor, M. Paulose and C. A. Grimes, *Adv. Funct. Mater.*, 2005, **15**, 1291.
- 5 S. S. Mali, P. S. Shinde, C. A. Betty, P. N. Bhosale, W. J. Lee and P. S. Patil, *Appl. Surf. Sci.*, 2011, **257**, 9737.
- 6 S. S. Mali, S. K. Desai, D. S. Dalavi, C. A. Betty, P. N. Bhosale and P. S. Patil, *Photochem. Photobiol. Sci.*, 2011, **10**, 1652.
- 7 H. R. Jhong, D. S. H. Wong, C. C. Wan, Y. Y. Wang and T. C. Wei, *Electrochem. Commun.*, 2009, **11**, 209.
- 8 S. H. Kang, J. Y. Kim, Y. Kim, H. S. Kim and Y. E. Sung, *J. Phys. Chem. C*, 2007, **111**, 9614.
- 9 T. Kasuga, M. Hiramatsu, A. Hoson, T. Sekino and K. Niihara, *Adv. Mater.*, 1995, **11**, 1307.
- 10 D. Gong, C. A. Grimes, O. K. Varghese, W. Hu, R. S. Singh, Z. Chen and E. C. Dickey, *J. Mater. Res.*, 2001, **16**, 3331.
- 11 X. Ren, T. Gershon, D. C. Iza, D. Munoz-Rojas, K. Musselman and J. L. MacManus-Driscoll, *Nanotechnology*, 2009, **20**, 365604.
- 12 S. Z. Chu, K. Wada, S. Inoue, S. I. Hishita and K. J. Kurashima, *J. Phys. Chem. B*, 2003, **107**, 10180.
- 13 K. Yoo, H. Choi and D. D. Dionysiou, *Chem. Commun.*, 2004, 2000.
- 14 E. R. Cooper, C. D. Andrews, P. S. Wheatley, P. B. Webb, P. Wormald and R. E. Morris, *Nature*, 2004, **430**, 1012.
- 15 Y. Zhou and M. Antonietti, *J. Am. Chem. Soc.*, 2003, **125**, 14960.
- 16 K. L. Ding, Z. J. Miao, Z. M. Liu, Z. F. Zhang, B. X. Han, G. M. An, S. D. Miao and Y. J. Xie, *J. Am. Chem. Soc.*, 2007, **129**, 6362.
- 17 K. S. Yoo, H. Choi and D. D. Dionysiou, *Catal. Commun.*, 2005, **6**, 259.
- 18 Y. Liu, J. Li, M. J. Wang, Z. Y. Li, H. T. Liu, P. He, X. R. Yang and J. H. Li, *Cryst. Growth Des.*, 2005, **5**, 1643.
- 19 T. Nakashima and N. Kimizuka, *J. Am. Chem. Soc.*, 2003, **125**, 6386.
- 20 T. Welton, *Chem. Rev.*, 1999, **99**, 2071–2083.
- 21 N. Yu, L. Gong, H. Song, Y. Liu and D. Yin, *J. Solid State Chem.*, 2007, **180**, 799.

-
- 22 H. Kaper, F. Endres, I. Djerdj, M. Antonietti, B. M. Smarsly, J. Maier and Y. S. Hu, *Small*, 2007, **3**, 1753.
- 23 X. Jia, W. He, X. Zhang, H. Zhao, Z. Li and Y. Feng, *Nanotechnology*, 2007, **18**, 075602.
- 24 S. Tian, H. Yang, M. Cui, R. Shi, H. Zhao, X. Wang and L. Zhang, *Appl. Phys. A: Mater. Sci. Process.*, 2011, **104**, 149.
- 25 K. Ding, Z. Miao, Z. Liu, Z. Zhang, B. Han, G. An, S. Miao and Y. Xie, *J. Am. Chem. Soc.*, 2007, **129**, 6362.
- 26 B. Liu and E. S. Aydil, *J. Am. Chem. Soc.*, 2009, **131**, 3985.
- 27 E. Hosono, S. Fujihara, K. Kakiuchi and H. Imai, *J. Am. Chem. Soc.*, 2004, **126**, 7790.
- 28 H. E. Wang, Z. Chen, Y. H. Leung, C. Luan, C. Liu, Y. Tang, C. Yan, W. Zhang, J. A. Zapien, I. Bello and S. T. Lee, *Appl. Phys. Lett.*, 2010, **96**, 263104.
- 29 V. Swamy and C. B. Muddle, *Appl. Phys. Lett.*, 2006, 89163118.
- 30 D. Bersani and P. P. Lottici, *Appl. Phys. Lett.*, 1998, **72**, 73.